Design and Test of an Intraoral Electrode Grid for Tongue High-Density Electromyography

Design and Test of an Intraoral Electrode Grid for Tongue High-Density Electromyography

Alberto Botter, *Member, IEEE*, Taian Vieira, Chiara Busso, Federica Vitali, Marco Gazzoni, and Giacinto L. Cerone, *Member, IEEE*

***Abstract*— Tongue motor function is crucial in a wide range of basic activities and its impairment affects quality of life. The electrophysiological assessment of the tongue relies primarily on needle electromyography, which is limited by its invasiveness and inability to capture the concurrent activity of the different tongue muscles. This work aimed at developing an intraoral grid for high-density surface electromyography (HDsEMG) to non-invasively map the electrical excitation of tongue muscles. We developed a grid of 4 × 8 electrodes deposited over an adhesive 8-μm thick polyurethane membrane. The testing protocol was conducted on 7 healthy participants and included functional tasks (vowels articulation and tongue movements) aimed at activating different regions of the tongue. The electrical stability of contact was assessed by measuring electrode-tongue impedances before and after the tasks. The spatial amplitude distribution of global EMG and single motor unit action potentials (MUAPs) was characterized. Electrode-tongue impedance magnitude showed no significant changes in the pre-post comparison (58±46kΩ vs. 67±58kΩ at 50Hz). Contact stability was confirmed by the quality of the signals that allowed to quantify spatiotemporal characteristics of muscle activation during the different tasks. The analysis of the spatial distribution of individual MUAPs amplitude showed that they were confined to relatively small areas on the tongue surface (range: 0.5cm^2 – 3.9cm^2). A variety of different spatiotemporal MUAP patterns, likely due to the presence of different muscle compartments with different fiber orientations, were observed. Our results demonstrate that the developed electrode grid enables HDsEMG acquisition from the tongue during functional tasks, thus opening new possibilities in tongue muscle assessment both at global and single motor unit level.**

***Index Terms*— Electrode technology, electromyography, motor unit, decomposition, speech, tongue muscles.**

I. Introduction

TONGUE motor function is essential in several physiological processes such as speech, swallowing, mastication, and respiration. These functions are ensured by a complex muscular system composed of various muscles and muscular compartments, with distinct anatomical and functional properties [1]. Tongue muscles are spatially organized in layered patterns spanning the internal-external direction, symmetrically with respect to the sagittal plane and can be categorized into two main families: extrinsic and intrinsic. Extrinsic muscles - genioglossus (GG), hyoglossus (HG), and styloglossus (SG) - have at least one attachment to a bone and are mainly responsible for tongue position changes, as defined in [1]. Conversely, intrinsic muscles - superior longitudinal (SL), transverse/vertical (T/V), and inferior longitudinal (IL) - have no bony attachments and their activation contributes predominantly to tongue shape changes. Pathologies affecting the central nervous system can disrupt the motor control of the tongue, leading to debilitating effects that impact diverse aspects of daily life, ranging from speech to food swallowing [2], [3], [4]. Similar functional impairments can arise from anatomical and physiological alterations due to injuries, oncological surgery and radiotherapy [5], [6], [7].

Characterizing the tongue muscles from a neuromechanical perspective is essential for assessing and rehabilitating specific motor functions. Over the past few decades, biomechanical models of tongue function have made significant contributions to understanding how various neural and physical factors interact in speech production [8], [9], [10], [11], [12]. However, the development of these models has not been supported by a corresponding advancement in experimental methodologies capable of providing input data or experimentally verifying model predictions. This observation applies particularly to neural aspects, which are crucial for understanding tongue motor control. Indeed, to date, the electrophysiological assessment of tongue muscles is mainly performed with intramuscular electromyography (iEMG, using either needle or wire electrodes) [13], [14] that exhibits evident limitations related to the patient discomfort and the

Manuscript received 31 May 2024; revised 8 July 2024; accepted 20 July 2024. Date of publication 29 July 2024; date of current version 8 August 2024. *(Corresponding author: Alberto Botter.)*

This work involved human subjects or animals in its research. Approval of all ethical and experimental procedures and protocols was granted by the Ethics Committee of the University of Turin under Application No. 260700.

Alberto Botter, Taian Vieira, Federica Vitali, Marco Gazzoni, and Giacinto L. Cerone are with the Laboratory for Engineering of the Neuromuscular System (LISiN), Department of Electronics and Telecommunications, and the PolitoBIOMed Laboratory, Politecnico di Torino, 10129 Turin, Italy (e-mail: alberto.botter@polito.it).

Chiara Busso is with the Division of Physical Medicine and Rehabilitation, Department of Surgical Sciences, University of Turin, 10124 Turin, Italy.

Digital Object Identifier 10.1109/TNSRE.2024.3434360

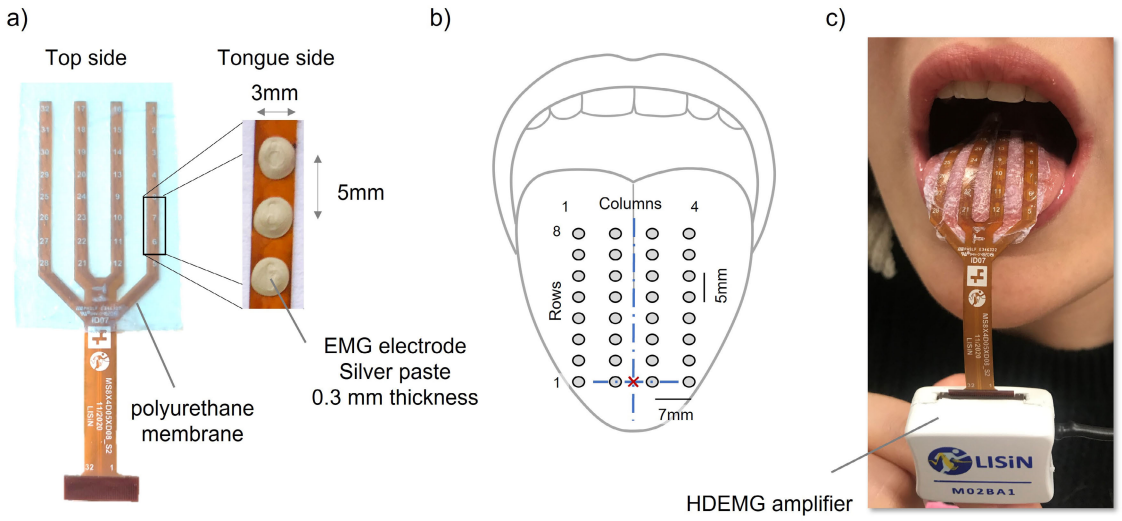

Fig. 1. a) The 4 × 8 grid of electrodes for tongue HDsEMG. Four mylar strips of 3 – mm width house the electrodes and the electrical connections. Individual electrodes are dome shaped (base diameter: 3 mm, height: 0.5 mm) and are obtained though the deposition of biocompatible silver ink. b) Schematic representation of the grid positioning on the tongue. The red cross represents the origin of the cartesian coordinate system used to analyse the spatial distribution of the detected signals. c) Picture of the grid positioned on the tongue and connected to the HDsEMG amplifier.

high spatial selectivity of the sampling. In fact, intramuscular electrodes usually employed in tongue studies are sensitive to electrical events occurring within an area of a few mm^2 in correspondence of the needle tip [15]. While this technique enables the accurate study of few individual motor units, its high spatial selectivity provides information limited to the muscle or muscle compartment where the needle is inserted. Given the large number of muscles composing the tongue and the differential spatial arrangement of their fibers, these characteristics represent a limitation when it is necessary to assess the coordinated activation of several tongue muscles during functional tasks. In this case, a less selective yet more representative sampling of the entire lingual muscle activity might be advisable.

As compared to iEMG, surface electromyography (sEMG) allows to detect myoelectric activity form a larger detection volume [16]. Furthermore, by using multiple electrodes on the muscle surface (high-density surface electromyography or HDsEMG), it is possible to non-invasively map muscle electrical activity across surfaces spanning several cm^2. This approach enables the investigation of how muscle activity is distributed in space among muscles and within muscle compartments, providing, in comparison with single channel detection, a more representative description of the neural input to the muscle(s) [17], [18]. Extensive literature demonstrates how the analysis of HDsEMG allows to reveal anatomical and physiological information, either at the muscle or at the motor unit level [19]. Given the complex arrangement of tongue muscles, the spatiotemporal mapping provided by HDsEMG could contribute to distinguish the different, abutting muscles and characterize their activation during motor tasks. To date, although some non-invasive detection systems have been proposed [20], [21], [22], [23], intraoral surface EMG form the tongue is limited to a single channel detection. This is mainly due to: (i) the technological challenge of obtaining a stable electrode contact during tasks demanding tongue shape changes, while preventing saliva from compromising the electrical contact properties; (ii) the lack of minimally invasive instrumentation used to acquire HDsEMG signals. While the latter limitation was partially overcame by the availability of wireless and miniaturized biopotential acquisition systems [24], the challenges related to the detection system design is still worth of investigation. The aim of this study is to develop an intraoral grid for HDsEMG detection and test for its potential in discriminating the regional changes in the distribution of tongue muscle excitation.

II. Methods

A. Electrode Grid Design

The design of the electrode grid was derived from prior insights into EMG spatial mapping of skeletal muscles and muscle compartments [17], [25], combined with specific considerations stemming from the unique characteristics of the intraoral environment. The need to arrange several electrodes on the tongue, without compromising its mobility led to the design of an electrode system with a few tens of surface electrodes distributed over an area of approximately 20 cm^2, covering the dorsal surface of the tongue. Additionally, the grid structure and its attachment to the tongue's surface were devised to accommodate basic tongue movements and fundamental functions, while ensuring mechanical and electrical stability for the time required to perform an electrophysiological evaluation of tongue, which has been estimated to take up to 20 minutes. A grid of 32 silver electrodes (4 columns x 8 rows) printed on a polyimide substrate was developed (Fig. 1a). Each column of electrodes was mechanically independent from the others and consisted of a thin (3 mm width) polyimide strip housing the electrical connections between the electrodes and the connector and acting as encapsulant layer. The electrodes were dome-shaped (base diameter: 3 mm, height: 0.5 mm) to improve the stability of the electrode-tongue contact. Electrodes were obtained by depositing a

silver ink (Dycotec DM-SIP-3060S, Dycotec materials Ltd, Calne, UK) on the electrical pads of the mylar strips with a 5mL syringe. The mylar structure was covered by a flexible polyurethane membrane (thickness: 8 μm) treated with a biocompatible adhesive to protect the electrical connection from saliva and secure the grid to the dorsal tongue surface.

B. In-Vivo Testing of the Grid

1) Experimental Protocol: The objectives of the experimental protocol were twofold. First, to verify the feasibility of HDsEMG acquisitions from the tongue, and second to assess the capability of the developed grid to characterize the spatiotemporal properties of global EMG and single motor unit action potentials during different motor tasks. Seven volunteers (age: 31 ± 5 years, height: 179 ± 4 cm, body mass: 72 ± 5 kg) were recruited for study purposes. No subject had any relevant ongoing neurological or other diseases that may alter muscle activity. The study was conducted in accordance with the Declaration of Helsinki and with the approval of the Ethics Committee of the University of Turin (Approval number: 260700 - 01/06/2022). The informed consent was obtained from all participants prior to the beginning of the study.

The study was conducted within a single experimental session that lasted approximately one hour. After drying the tongue surface with a tissue, the grid of electrodes was positioned on the dorsal surface of the tongue. The impedance between consecutive electrodes of the grid was measured to evalua 7-10 minutes. Afterwards, surface electromyographic signals were detected during articulation of the vowels /a/, /i/, /u/, and the tongue retraction, in this fixed order. During tongue retraction participants were asked to limit the superior bending of the tongue tip (see Fig. 5 in [1]). These tasks were selected to activate different regions of the tongue while inducing moderate alterations in tongue shape [1], [9], [13]. Each task was executed for a duration of 20s, with 30 s rest periods between consecutive tasks. After tongue retraction, participants were engaged into conversation, demanding pronunciation of brief words until 20 minutes had passed since the application of the grid. Subsequently, the impedance of the electrodes was measured to assess the capability of the grid to maintain a stable contact also after stress caused by the tongue movements.

Participants were allowed to swallow saliva at any time during the experiment, and no saliva aspirator was utilized during the experimental protocol.

2) Electrode-Tongue Impedance Measure and Analysis: The electrical impedances between consecutive electrodes of each column of the grid were measured at 50 Hz (Power Line frequency) [26] before ($|Z50|_B$) and after ($|Z50|_E$) the motor tasks. Impedances were measured with a custom-made impedance meter (LISiN, Politecnico di Torino, Italy). This device converts a sinusoidal voltage input into a proportional current signal (200 nA peak-to-peak amplitude) and measures the voltage drop between the electrodes tested. Both the sine wave, used to drive the current signal, and the voltage drop were sampled with a National Instrument data acquisition device (USB-6210, sampling frequency:10 kHz, resolution of the A/D converter: 16 bits). The magnitude of the impedance was quantified as the ratio between the measured voltage and injected current at 50 Hz [27]. The number of channels displaying an impedance larger than 1MΩ were regarded as missing contacts [27], [28].

TABLE I
MAGNITUDE OF THE ELECTRODE-TONGUE IMPEDANCES AT 50 HZ AND NUMBER OF MISSING CONTACTS AT THE BEGINNING ($|Z50|_B$) AND AT THE END ($|Z50|_E$) OF THE EXPERIMENTAL SESSION

Subj#	$\|Z50\|_B$ (kΩ)	$\|Z50\|_E$ (kΩ)	$\|Z50\|_B$ > 1MΩ	$\|Z50\|_E$ > 1MΩ
1	19.9 (13.0 – 87.1)	10.3 (7.2 – 27.2) §	2	2
2	27.3 (22.7 – 29.8)	18.0 (8.6 – 23.9) §	0	0
3	13.8 (11.5 – 21.0)	7.1 (6.6 – 16.2) §	0	0
4	30.2 (10.8 – 60.4)	27.5 (16.1 – 46.9) *	0	0
5	30.6 (22.5 – 38.4)	27.9 (23.7 – 43.1) §	0	2
6	26.2 (15.7 – 35.1)	19.3 (10.2 – 24.7) §	0	0
7	37.4 (11.7 – 83.5)	30.8 (9.7 – 68.8) §	0	0
Pooled data	24.7 (13.4 – 45.7)	20.0 (8.0 – 35.9) §		

Wilcoxon signed rank test p<0.05 (*), p<0.001 (§).

3) HDsEMG Detection and Analysis: EMG signals were detected in monopolar configuration using a wireless and miniaturized high-density EMG amplifier (MEACS - LISiN, Politecnico di Torino, Italy and ReC Bioengineering Laboratories, Turin, Italy) [29]. The reference electrode for monopolar recordings was positioned behind the right ear on the mastoid process. Signals were amplified (192 V/V), band-pass filtered (10 Hz -500 Hz), sampled at 2048 Hz, digitalized with a 16 bits A/D converter and transmitted through a Wi-Fi link to a personal computer for real-time visualization and storage. Offline analysis was performed with Matlab (version R2023a; The Math-Works, Natick, MA, USA). Signals were band-pass filtered with a second-order Butterworth filter (20–400 Hz cutoff frequencies) and visually inspected to identify bad channels, i.e. channels showing unstable baseline or high level of power line interference due to a non-optimal electrode-tongue contact. Bad channels (2 out of 32 at most, see Table I) were either removed and interpolated with neighbor channels or cleaned with filtered-virtual reference method [30].

The root mean square (RMS) amplitude was computed for each monopolar channel of the grid and used to describe the spatial distribution of EMG amplitude over the tongue surface. After interpolating the RMS maps with a factor 4, the size of the tongue surface providing greatest EMG signals was defined by segmenting the interpolated RMS map. This *segmented area* was defined as the sum of the areas of the interpolated channels providing an RMS amplitude higher than 70% of the maximum. The barycenter of the RMS maps was used to describe the location of the identified area. A cartesian coordinate system with the origin in correspondence to the intersection between row 1 (most external row, Fig. 1) and the midline between columns 2 and 3 was used to define the barycenter coordinates.

HDsEMG signals were then decomposed into their constituent motor unit action potential trains using a validated, semi-automated algorithm based on Convolutive Kernel Compensation [31], [32]. The spike trains were manually edited,

and MU action potentials (MUAPs) were computed through spike trigger averaging over the edited spike trains. The quality of identified MUs from HDsEMG was quantified using the Pulse-to-Noise Ratio (PNR) and the MUAP spatiotemporal properties [33], [34]. The RMS distribution of MUAP amplitude was used to characterized MUAPs in terms of area occupied on the tongue surface (*MUAP segmented area*) and barycenter, using the same approach adopted for global EMG signal analysis. Furthermore, the alignment between muscle fibers generating the decomposed MUAPs and the columns of electrodes was assessed through the conduction velocity (CV). MUAPs were detected from fibers deemed to be parallel to the columns of electrodes when CV estimates fell within the physiological range of 2-6 m/s [35]. MUAPs exhibiting conduction velocities within this physiological range were categorized as *propagating potentials*, whereas those falling outside this range were classified as *non-propagating potentials.* It is worth noting that 'propagating' and 'non-propagating' potentials refer to the electrical potentials measured by the EMG detection system on the tongue surface. These electrical potentials are associated with action potentials, which always propagate along the muscle fibers. However, they may appear as either propagating waves or not, depending on the alignment between the electrodes and the muscle fibers [17].

C. Statistical Analysis

Wilcoxon signed rank test was used to compare the magnitude of the electrode-tongue impedances measured at the beginning ($|Z50|_B$) and at the end ($|Z50|_E$) of the experimental protocol. The effect of the motor task on the spatial distribution of global EMG activity on the tongue surface (x and y coordinates of the distribution's barycenter, size of the segmented area) was tested with Friedman's ANOVA followed by post-hoc comparisons with Bonferroni correction. Mann Whitney test was used to compare the spatial distributions (x and y coordinates of the distribution's barycenter) of propagating and non-propagating MUAP. All statistical tests were performed in Matlab (version R2023a; The Math-Works, Natick, MA, USA). The threshold for statistical significance was set at $p < 0.05$ for all comparisons. Results are reported as *median (first quartile – third quartile)*.

III. Results

None of the participants reported discomfort or pain during and after all phases of the experiment, including attachment or detachment of the grid. Possible adhesive residues remaining on the tongue surface, were removed by gently scraping the tongue with a toothbrush and rinsing the mouth after the experiment.

A. Electrode-Tongue Impedance

Table I reports the median and inter-quartile range of the electrode-tongue impedance values of the 32 electrodes at the beginning ($|Z50|_B$) and at the conclusion ($|Z50|_E$) of the experimental session. A statistically significant reduction of electrode-tongue impedance was observed ($|Z50|_B$ = 24.7 (13.4 – 45.7) kΩ vs $|Z50|_E$ = 20.0 (8.0 – 35.9) kΩ; $p < 0.001$, Wilcoxon signed rank test). This reduction is further shown by the scatterplot reported in Fig. 2. The number of missing contacts before and after the motor tasks (last two columns of Table I) confirms the quality of the electrodes' contact throughout the entire experiment.

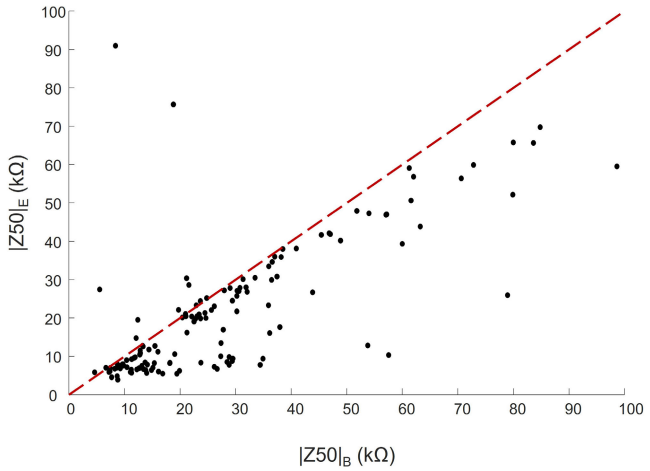

Fig. 2. Magnitude of the electrode-tongue impedance at 50 Hz measured before ($|Z50|_B$) and after ($|Z50|_E$) the motor tasks. The scatterplot reports the values lower than 100kΩ, representing respectively 91% and 95% of $|Z50|_B$ and $|Z50|_E$ distribution sizes.

B. Global HDsEMG Variables

EMG activity distributed unevenly over the tongue surface during the considered motor tasks. Fig. 3b shows four representative examples of monopolar EMG signals and their RMS spatial distributions during the articulation of the vowels /a/, /i/, /u/ and during tongue retraction. Different locations of the active regions in the longitudinal tongue direction were observed for different tasks. When considering all participants (Fig. 3c), the longitudinal coordinate of barycenter of the EMG distribution changed significantly ($p < 0.05$) for the four tasks (vowel /a/: 13.6 (12.5 - 14.8) mm, vowel /i/: 15.0 (14.5 - 16.7) mm, vowel /u/: 17.3 (16.4 - 19.3) mm, and retraction: 19.5 (17.3 - 20.7) mm, Fig. 3c), indicating a shift of the EMG distribution from the anterior (0 mm) to the posterior part of the tongue. The transversal coordinate of the EMG distribution barycenter did not change significantly across the tasks ($p = 0.16$) and was centered in the longitudinal axis of the tongue (grand average: 0.1 (−0.38 - 0.40) mm, Fig. 3c). The size of the segmented areas was 1.3 (1.0 – 2.1) cm^2 (values computed across participants and tasks) and did not change significantly across the tasks ($p = 0.06$) (Fig. 3c).

C. Single Motor Unit Characterization

A total of 116 MUs were identified across all the participants. The number of MU identified per contraction was 3 (2 – 5), the average PNR was 28 (26 – 30.2) dB, the firing rate was 19 (16 – 22) pps. Fig. 4a depicts the firing pattern of a representative signal (vowel /i/). The analysis of the spatiotemporal evolution of action potentials showed that both *propagating* and *non-propagating potentials* are concurrently present on the tongue surface during all motor tasks. Fig. 4

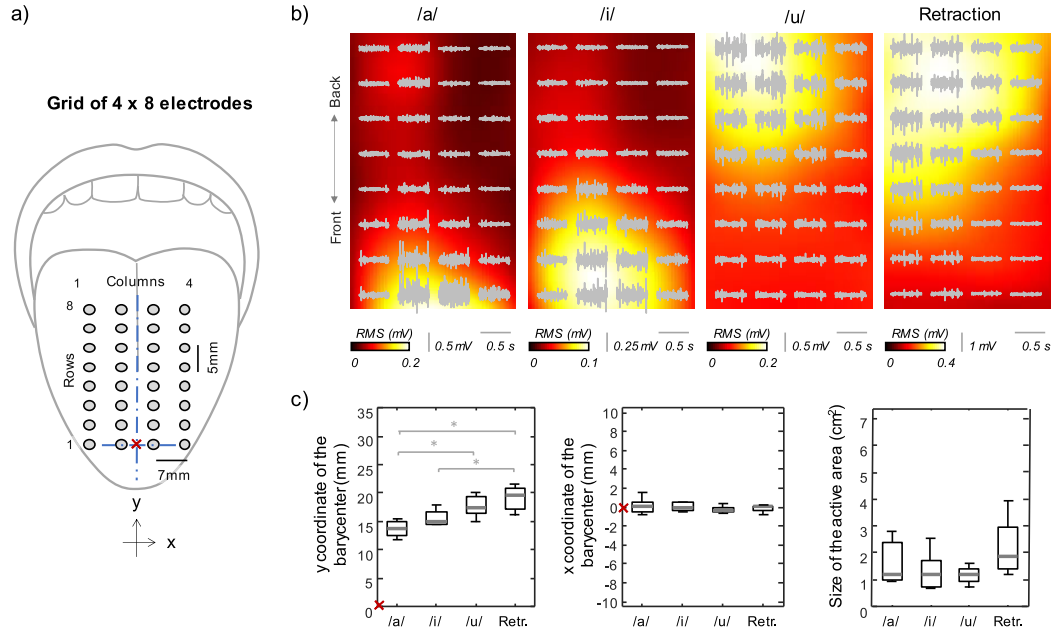

Fig. 3. a) Schematic representation of the grid positioning on the tongue. The red cross represents the center of reference system $(x, y) = (0, 0)$ - for the barycenter coordinates. b) RMS amplitude distribution of the monopolar EMG activity for different tasks in one representative participant. From left to right: articulation of the vowel /a/, / i/, /u/ and tongue retraction. Monopolar EMG signals detected by each channel of the grid are superimposed to the amplitude maps. c) x and y coordinates of the barycenter of the RMS maps and size of the segmented area for each task (N = 7 subjects). (*$p < 0.05$).

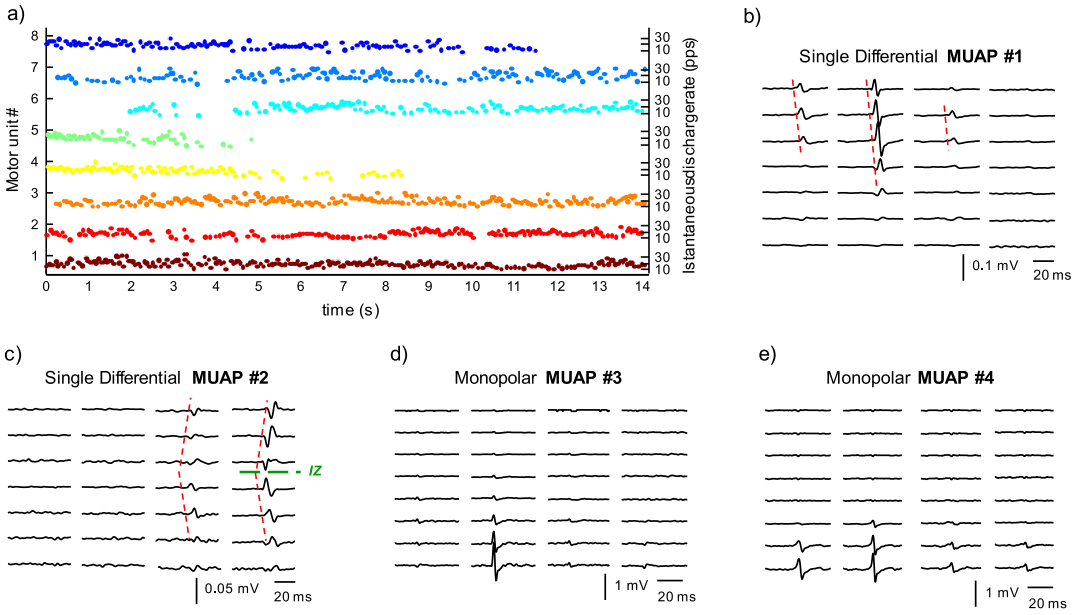

Fig. 4. Motor Unit (MU) identification in a representative participant. a) instantaneous firing rate of 8 MUs during the sustained articulation of the vowel /i/. b) c) d) e) Four examples of motor unit action potentials (MUAPS) showing different spatiotemporal properties. Red-dotted lines indicate the propagation of single differential MUAP #1 and #2 (IZ: innervation zone). No propagation was observed in MUAPs #3 and #4, displayed in monopolar configuration. Note the clear differences in MUAP shape and location for each of the identified units.

reports four examples of MUAPs with different spatiotemporal properties within the same contraction in an individual subject. MUAP#1 and MUAP#2 show a clear propagation highlighted by red-dotted lines in Fig. 4b,c. MUAP#2 shows the typical V-shape propagation pattern [36] arising from the innervation zone (IZ). This pattern was not observed in MUAP#1, where the innervation zone is likely outside the region covered by the grid. In both cases single differential MUAPs are reported to highlight the propagating component that would be less visible in monopolar configuration [37]. MUAP #3 and MUAP #4 are non-propagating potentials that are spatially represented in correspondence of the tongue tip, either in a narrow area (MUAP #3) or in a wider area spanning the whole width of the grid (MUAP 4#).

Taking into account the entire decomposed dataset, individual MUAPs were represented over a restricted number of

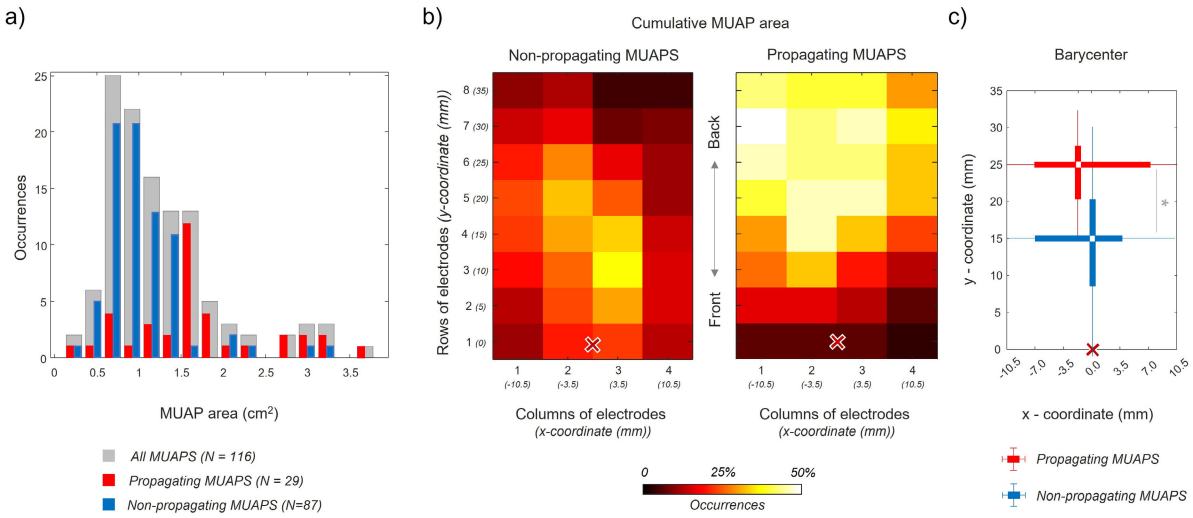

Fig. 5. Size and location of the identified MUAPs. a) Distribution of the size of monopolar MUAP segmented areas. b) cumulative spatial distribution of the MUAP segmented areas (left map: non-propagating MUAPs (N = 87); right map: propagating MUAPs (N = 29)). The heatmaps indicate the percentage of MUAPs represented in each channel of the grid. c) Barycenter of propagating (red) and non-propagating (blue) MUAP segmented areas (*: $p < 0.001$ Mann-Whitney test). The red cross is the center of the reference system - (x, y) = (0, 0) - for the barycenter coordinates.

channels, spanning from 2 to 17 (i.e. from 0.5 cm^2 to 3.9 cm^2, considering a total area of 7.4 cm^2 covered by the 32 channels grid). The distribution of MUAP spatial dimension was skewed towards low values (median = 1.2 cm^2; i.e. 5 channels), as shown in Fig. 5a (grey bars). Considering all decomposed MUAPs, 25% were propagating potentials and 75% did not show any propagation. On average, the conduction velocity of propagating MUAPs was 3.5 (2.9 – 4.2) m/s. Propagating and non-propagating potentials were distributed differently over the tongue surface, with the former occupying a larger region in the internal-external direction compared to the latter (20 (14 - 25) mm vs 10 (5 - 15) mm, $p < 0.001$ Mann-Whitney test). Moreover, propagating MUAPs predominantly located toward the posterior region, while non-propagating MUAPs were more evenly dispersed across the tongue surface (Fig. 5b). These distributions led to statistically significant differences in the longitudinal coordinates of the MUAPs' barycenter (25 (10 – 17.5) mm for propagating potentials vs 15.5 (8 - 20.5) mm for non-propagating potentials, being 0 mm the most external electrode, $p < 0.001$ Mann-Whitney test), while no statistically significant differences were observed in the transversal coordinates of the MUAP barycenter (Fig. 5c).

IV. Discussion

In this study we developed and tested an intraoral grid for HDsEMG recordings to map the electrical activation of tongue muscles during functional tasks. Experimental results revealed good contact stability throughout the motor tasks enabling the characterization of the spatial distribution of global EMG activity over the tongue surface. Furthermore, we showed the possibility to assess the firing characteristics of individual motor units as well as the spatiotemporal properties of their action potentials. The analysis of both global and single motor unit EMG showed a variety of spatial activation patterns presumably associated with the activity of different tongue muscles. The results of the current study prove the feasibility of tongue HDsEMG detection, providing a new tool for the investigation of this complex muscle group.

The approaches previously used in literature to investigate the electrophysiological properties of tongue muscles are based on needle electrodes [13], [14], bipolar surface electrodes positioned on the surface of the tongue [20], [21], [23], or multichannel surface electrodes placed externally in the submental region [23]. If the objective is to study the coordinated activation of tongue muscles, all these approaches present potential limitations that restrict their applicability: invasiveness (needle electrodes), poor spatial selectivity of measurement (bipolar electrodes positioned on the surface of the tongue), and the presence of other muscles not belonging to the tongue in the sampling volume (externally placed electrodes). In this context, the use of a multi-channel approach to EMG signal acquisition aims to address and overcome these limitations, providing a valuable tool for studying the activation of a highly complex muscle group in terms of anatomy, movement, and control.

The measurement of HDsEMG signals from the surface of the tongue poses various technological challenges, primarily related to the quality and stability of electrical contact. The technological solution proposed in this work allowed to achieve a good compromise between the temporal stability of electrical contact and the tongue's mobility necessary to perform simple tasks. The technology presented in this study builds upon standard grid technology using flexible PCBs [38], [39] with specific innovations. Unlike traditional technology, it does not require bi-adhesive pads and conductive gel between the electrodes and the skin. Instead, it utilizes dome-shaped electrodes to enhance dry contact and incorporates a thin and flexible PCB design with independent columns, allowing the grid to conform to the tongue's shape changes. Additionally, an external membrane protects the sampling system from saliva infiltration, which could degrade both the mechanical and electrical interface with the tongue.

Recent literature has proposed other solutions based on thin films or polymer composites electrodes [40], [41] that may be employed in tongue EMG. Although these technologies provide highly conformable electrodes, at present, their fabrication processes are often complex and expensive, and the electrode characteristics (size, behavior in wet environment) may not be adequate for this specific application. Moreover, interfacing with the front-end electronics can be challenging due to the coupling between the soft film support and the rigid electronic connectors. While these issues do not compromise electrode usability in well controlled, laboratory conditions, currently they may result in a limited practical usability in applied contexts requiring tongue EMG detection. In this study, we opted for a more conservative approach that allowed to achieve a device with good performance in terms of mechanical adhesion and signal quality, while also utilizing standard production processes and ensuring immediate usability.

The quality of electrical contact between electrodes and tongue was assessed through the measurement of the electrode-tongue impedance magnitude, and further confirmed by the quality of the detected signals. Electrical impedances between electrodes and tongue were stable throughout the tests and comparable to those of gelled electrodes with similar sizes positioned over the skin [26]. This evidence can likely be attributed to the wet environment that improves the electrode-tongue contact allowing to reach relatively low impedance values even without the use of conductive gel. It is important to note that in this study we measured the impedance between two exploring electrodes of the grid, meaning that the reported impedance values included two electrode-tongue interfaces as well as the impedance of the interposed tissue (often considered negligible [26]). Therefore, assuming that the two electrode-tongue interfaces have similar impedances, the impedance of single electrodes is approximately half the reported values [27]. The impedance measurement between pairs of exploring electrodes was used because it enables the identification of short circuits or low impedance paths between consecutive electrodes. This occurrence, which may arise from saliva infiltration under the grid, represents a particularly significant issue in tongue EMG, as it can result in the attenuation of single differential signals and consequently affect the accuracy of amplitude estimation. After 20 minutes we observed an overall reduction of the electrode-tongue impedance (Table I and Fig. 2) and a negligible number of missing contacts (last two columns of table I), indicating good quality and stability of the tongue-grid contact. It is worth noting that when the impedance is measured between two exploring electrodes, a single missing electrode-tongue contact will result in two high impedance values ($|Z50| > 1M\Omega$ in table I), unless the missed contact is in the most internal or external row (rows 1 and 8). Our electrodes showed a good electrical contact throughout the experiments, with just one missing contact in participants 1 and 5 (table I). The observed reduction of impedance with time from the electrodes' application is in line with previous studies on electrode-skin contact [26]. These results suggest it could be a good practice starting EMG acquisition after few minutes from the grid positioning, although further studies focused on the time course of impedance reduction are required to provide more detailed indications.

The quality of electrical contact between the grid and the tongue was confirmed by the analysis of the signals detected during the motor tasks. The study of EMG spatial distribution during the articulation of vowels /a/, /i/, /u/, and tongue retraction highlighted different activation patterns (Fig. 3) that are consistent with tongue anatomy and previous evidence from in-vivo and in-silico studies [1], [9], [13]. Specifically, the observed progressive shift of the center of mass towards the central-posterior part of the tongue for the vowels /a/, /i/, and /u/ is in line with the hypothesis of a modulation of the relative activation of anterior and posterior muscles of the tongue. For example, the activity of the anterior genioglossus is required to limit the rotation of the apex and the elevation of the tongue in vowels /a/ and /i/ respectively, whereas the posterior genioglossus contributes to increasing the size of the vocal tract in high vowels like /i/ and /u/ [9], [13]. Although, several other muscles contribute to vowels articulation and the maintenance of tongue shape [9], the described activation pattern is consistent with the observed spatial shift of EMG. Regarding the retrusion task, it is mainly performed by extrinsic muscles (hyoglossus, and styloglossus that are not sampled by our grid of electrodes); however, the associated tongue shortening is likely due to the action of the muscles that are oriented lengthwise, primarily the superior (SL) and inferior longitudinal (IL) [1] While the IL is deep and its contribution to surface EMG may be limited, SL is superficial and its fibers run parallel to the tongue superior surface, mainly in the central-posterior tongue regions, which is consistent with an EMG distribution reported in Fig. 3. These results demonstrate that the developed system is capable of revealing different spatial patterns of activation associated with the activation of different tongue muscles. This evidence suggests the potential of spatial mapping of the EMG signal for identifying active muscles during a motor task for basic or applied studies (e.g., follow-up after tongue surgery, biofeedback in rehabilitation protocols). It is important to note that the experimental protocol was not devised to study the activity of specific muscles, but only to demonstrate that it was possible to capture spatial heterogeneity and how this varied for different motor tasks. For instance, the frequency of the emitted sound was not controlled, and normalization with respect to tongue size was not performed, which are aspects to control to study individual muscles' activation in a subject population.

The decomposition of HDsEMG signals has demonstrated the feasibility of single motor unit analysis from tongue muscles. The analysis of the spatial distribution of MUAPs revealed that the electrical activity of individual MUs is represented locally on the tongue surface. MUAP segmented areas of few square centimeters were observed both in one side of the tongue surface (e.g., MUAP#2 in Fig. 4) and symmetrically to the longitudinal axis (e.g., MUAP#4 in Fig. 4). This is consistent with innervation patterns described in the literature [42] and with the muscular anatomy of the tongue, comprising several layers of muscles, each with

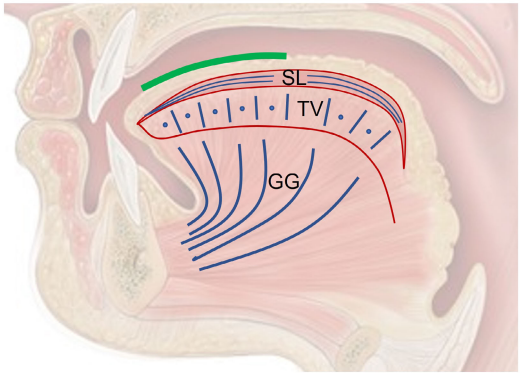

Fig. 6. Representation of the sagittal section of the tongue. The Superior Longitudinalis (SL) muscle extends along the length of the tongue, with fibers aligned longitudinally to the superior surface. The thickness of the SL muscle diminishes towards the tongue tip. Below the SL muscle lies the Transverse-Vertical (TV) muscle, with fibers oriented on the coronal plane in vertical and transverse directions (the latter are indicated by blue dots). Genioglossus (GG) muscle is deeper and its fibers organized in a fan-like structure. The approximate position of the HDsEMG grid is indicated by the green thick line on the tongue surface.

specific functions and fiber orientations [1]. The association between the identified MUAPs and the muscles to which the MU belongs is challenging and cannot be systematically verified with the methodologies used in this study. However, associations can be hypothesized based on the spatiotemporal MUAP characteristics (presence or absence of propagation) and the knowledge on the anatomy of intrinsic tongue muscles. Indeed, it is known that the ability to observe propagating potentials depends on the relative orientation between muscle fibers and surface electrodes [17]. The tongue contains several muscles with different fascicle architectures whose combined action enables the complex tongue shape changes necessary to perform motor tasks (see Fig. 3 in [1]). For example, the SL muscle spans the length of the tongue with fibers aligned longitudinally to the superior surface, the vertical-transverse muscle has fibers positioned on the coronal plane in vertical and transverse directions, and the genioglossus muscle has a fan-like structure (Fig. 6). Propagation of the potential along the longitudinal axis could therefore be associated with the activation of SL muscle fibers. Instead, non-propagating potentials may be due to activity of the vertical or genioglossus muscles, whose fibers not aligned with the tongue surface (Fig. 6) and generate, on the electrode plane, the typical MUAP pattern of in depth-pinnate muscles [17]. The spatial characteristics of the segmented areas of propagating and non-propagating potentials seem to confirm this interpretation. Indeed, segmented areas of propagating potentials are larger, elongated longitudinally (the propagation direction in SL) and centered in a more posterior position, where the SL muscle is thicker [1]. Instead, territories of non-propagating potentials are more localized in the anterior part of the tongue (Fig. 5 and 6). In this region, the thickness of the SL muscle decreases, and the fibers of the vertical and genioglossus muscles terminate closer to the tongue surface, resulting in larger potentials detected by anterior electrodes (Fig. 6). Although further analysis and studies are required, these considerations highlight the potential of tongue HDsEMG in distinguishing the activation of different muscular structures in various areas of the tongue, which may find relevant applications in basic and applied research.

The proposed grid of electrodes improves the existing technologies for the electrophysiological characterization of the tongue, enabling non-invasive investigations of tongue function and control. However, it is important to highlight some limitations of the proposed technology. First, while the conformability of the grid makes it suitable for the considered tasks that induce moderate tongue shape changes, it may not be adequate for more complex shape changes. The conformability of our detection system is mainly in one direction (the transversal direction, where columns of electrodes are independent), while shape changes in the internal-external direction are limited by the inelastic polyimide substrate. Furthermore, it is worth noting that the higher IED in the internal-external direction compared to the transverse direction was designed considering the expected symmetrical activation of the tongue around the sagittal plane for the considered motor task. However, if there is an interest in studying mediolateral asymmetries in tongue activation with higher spatial resolution in the transvers direction, it is possible to modify the electrode configuration using the same technological approach presented in this study. Another limitation to note is that this study did not include a rigorous mechanical characterization of the grid's adhesion. Due to the unavailability of methods to perform these evaluations in vivo, we opted for an indirect method based on the assumption that the lack of mechanical contact between the membrane and the tongue would inevitably lead to saliva infiltration under the electrodes, resulting in short circuits between adjacent electrodes. The fact that the electrode-tongue impedance assessment did not show short circuits, suggests that the mechanical adhesion was sufficiently good for the motor tasks considered.

Finally, various applications can be envisioned for the proposed grid of electrodes. Structural and functional tongue changes impairing swallowing and speaking abilities are common in several patient populations, such as those affected by pathologies (e.g. motor neuron disorders), individuals affected by central or peripheral trauma, and patients whose tongue anatomy and function has been altered due to oral cancer surgery or chemotherapeutic or radiation treatments. A better understanding of tongue muscle activation during functional tasks can contribute, together with other methodologies - e.g. imaging techniques, kinematic measures, strength assessments, biomechanical models - to refine rehabilitation protocols, monitor changes linked to pathology development and progression, and predict functional impairments such as those resulting from surgery or resection of specific tongue regions [43]. Furthermore, it is worth noting that the tongue is a target muscle for the assessment of neuromuscular alterations and for the identification of fasciculation potentials in amyotrophic lateral sclerosis (ALS) [44], [45], [46], [47]. HDsEMG has demonstrated feasibility in improving fasciculation sensitivity [48], [49], [50], and within this context, our proposed electrode system finds application in the non-invasive identification and classification of fasciculation potentials originating from various tongue muscles.

Conflicts of Interest

The authors Alberto Botter, Taian Vieira, Marco Gazzoni, and Giacinto L. Cerone are involved in the activities of ReC Bioengineering Laboratories, a spin-off of the Laboratory for Engineering of the Neuromuscular System (Politecnico di Torino), which produces and commercializes devices for neuromuscular system assessment. The findings described in this article are not intended to promote any product or services of the company.

Acknowledgment

The authors are grateful to Prof. Marco Alessandro Minetto (Division of Physical Medicine and Rehabilitation, Department of Surgical Sciences, University of Turin, Turin, Italy) for his careful review of the final version of the manuscript.

References

[1] I. Sanders and L. Mu, "A three-dimensional atlas of human tongue muscles," *Anatomical Rec.*, vol. 296, no. 7, pp. 1102–1114, Jul. 2013, doi: 10.1002/ar.22711.

[2] B. J. Perry, K. L. Stipancic, R. Martino, E. K. Plowman, and J. R. Green, "Biomechanical biomarkers of tongue impairment during swallowing in persons diagnosed with amyotrophic lateral sclerosis," *Dysphagia*, vol. 36, no. 1, pp. 147–156, Feb. 2021, doi: 10.1007/s00455-020-10116-z.

[3] B. B. Recasens et al., "Ultrasonographic and manometric study of the tongue as biomarkers of dysphagia in patients with amyotrophic lateral sclerosis," *Neurological Sci.*, vol. 44, no. 3, pp. 931–939, Mar. 2023, doi: 10.1007/s10072-022-06486-x.

[4] S. Mathis et al., "Clinical neurology in practice," *Neurologist*, vol. 29, no. 1, pp. 59–69, Jan. 2024, doi: 10.1097/nrl.0000000000000510.

[5] S. Rios-Gonzalez, S. Heredero-Jung, J. Ruiz-Masera, and A. Martínez-Sahuquillo-Marquez, "Quality of life and functional outcomes in tongue cancer patients: A long-term, prospective, comparative study," *Medicina Oral Patología Oral Y Cirugia Bucal*, vol. 1, pp. e232–e240, Sep. 2024, doi: 10.4317/medoral.26228.

[6] M. E. M. C. Christianen et al., "Patterns of long-term swallowing dysfunction after definitive radiotherapy or chemoradiation," *Radiotherapy Oncol.*, vol. 117, no. 1, pp. 139–144, Oct. 2015, doi: 10.1016/j.radonc.2015.07.042.

[7] L. Van den Steen et al., "Evolution of self-perceived swallowing function, tongue strength and swallow-related quality of life during radiotherapy in head and neck cancer patients," *Head Neck*, vol. 41, no. 7, pp. 2197–2207, Jul. 2019, doi: 10.1002/hed.25684.

[8] Y. Payan and P. Perrier. (1997). *Synthesis of V-V Sequences With a 2D Biomechanical Tongue Model Controlled by the Equilibrium Point Hypothesis '*. [Online]. Available: https://www.elsevier.nl/locate/specom

[9] S. Buchaillard, P. Perrier, and Y. Payan, "A biomechanical model of cardinal vowel production: Muscle activations and the impact of gravity on tongue positioning," *J. Acoust. Soc. Amer.*, vol. 126, no. 4, pp. 2033–2051, Oct. 2009, doi: 10.1121/1.3204306.

[10] P.-Y. Rohan, C. Lobos, M. A. Nazari, P. Perrier, and Y. Payan, "Finite element models of the human tongue: A mixed-element mesh approach," *Comput. Methods Biomechanics Biomed. Eng. Imag. Visualizat.*, vol. 5, no. 6, pp. 390–400, Nov. 2017, doi: 10.1080/21681163.2015.1105760.

[11] Q. Fang, S. Fujita, X. Lu, and J. Dang, "A model-based investigation of activations of the tongue muscles in vowel production," *Acoust. Sci. Technol.*, vol. 30, no. 4, pp. 277–287, 2009, doi: 10.1250/ast.30.277.

[12] V. Sanguineti, R. Laboissière, and D. J. Ostry, "A dynamic biomechanical model for neural control of speech production," *J. Acoust. Soc. Amer.*, vol. 103, no. 3, pp. 1615–1627, Mar. 1998, doi: 10.1121/1.421296.

[13] T. Baer, P. Alfonso, and K. Honda, "Electromyography of the tongue muscles during vowels in/@pVp/environment," *Ann. Bull. RILP*, vol. 22, pp. 7–19, Aug. 1988.

[14] B. L. Luu et al., "Genioglossus motor unit activity in supine and upright postures in obstructive sleep apnea," *Sleep*, vol. 43, no. 6, pp. 1–28, Jun. 2020, doi: 10.1093/sleep/zsz316.

[15] E. Stlberg and B. Falck, "The role of electromyography in neurology," *Electroencephalogr. Clin. Neurophysiology*, vol. 103, no. 6, pp. 579–598, Dec. 1997.

[16] P. A. Lynn, N. D. Bettles, A. D. Hughes, and S. W. Johnson, "Influence of electrode geometry on bipolar recordings of the surface electromyogram," *Med. Biol. Eng. Comput.*, vol. 16, no. 6, pp. 651–660, Nov. 1978, doi: 10.1007/bf02442444.

[17] T. M. Vieira and A. Botter, "The accurate assessment of muscle excitation requires the detection of multiple surface electromyograms," *Exerc. Sport Sci. Rev.*, vol. 49, no. 1, pp. 23–34, 2021.

[18] K. Roeleveld, D. F. Stegeman, H. M. Vingerhoets, and A. V. Oosterom, "The motor unit potential distribution over the skin surface and its use in estimating the motor unit location," *Acta Physiologica Scandinavica*, vol. 161, no. 4, pp. 465–472, Nov. 1997, doi: 10.1046/j.1365-201x.1997.00247.x.

[19] R. Merletti and D. Farina, *Surface Electromyography: Physiology, Engineering, and Applications*. Hoboken, NJ, USA: Wiley, 2016.

[20] K. Yoshida, K. Takada, S. Adachi, and M. Sakuda, "Clinical science: EMG approach to assessing tongue activity using miniature surface electrodes," *J. Dental Res.*, vol. 61, no. 10, pp. 1148–1152, Oct. 1982, doi: 10.1177/00220345820610100701.

[21] C. M. O'Connor et al., "Improved surface EMG electrode for measuring genioglossus muscle activity," *Respiratory Physiol. Neurobiol.*, vol. 159, no. 1, pp. 55–67, Oct. 2007, doi: 10.1016/j.resp.2007.05.011.

[22] E. A. Doble, J. C. Leiter, S. L. Knuth, J. A. Daubenspeck, and D. Bartlett, "A noninvasive intraoral electromyographic electrode for genioglossus muscle," *J. Appl. Physiol.*, vol. 58, no. 4, pp. 1378–1382, Apr. 1985, doi: 10.1152/jappl.1985.58.4.1378.

[23] M. Sasaki et al., "Tongue interface based on surface EMG signals of suprahyoid muscles," *ROBOMECH J.*, vol. 3, no. 1, p. 9, Dec. 2016, doi: 10.1186/s40648-016-0048-0.

[24] G. L. Cerone and M. Gazzoni, "A wireless, minaturized multi-channel sEMG acquisition system for use in dynamic tasks," in *Proc. IEEE Biomed. Circuits Syst. Conf. (BioCAS)*, Oct. 2017, pp. 1–4, doi: 10.1109/BIOCAS.2017.8325129.

[25] A. Gallina et al., "Consensus for experimental design in electromyography (CEDE) project: high-density surface electromyography matrix," *J. Electromyogr. Kinesiol.*, vol. 64, Jun. 2022, Art. no. 102656, doi: 10.1016/j.jelekin.2022.102656.

[26] G. Piervirgili, F. Petracca, and R. Merletti, "A new method to assess skin treatments for lowering the impedance and noise of individual gelled Ag–AgCl electrodes," *Physiological Meas.*, vol. 35, no. 10, pp. 2101–2118, Oct. 2014, doi: 10.1088/0967-3334/35/10/2101.

[27] G. L. Cerone, A. Botter, T. Vieira, and M. Gazzoni, "Design and characterization of a textile electrode system for the detection of high-density sEMG," *IEEE Trans. Neural Syst. Rehabil. Eng.*, vol. 29, pp. 1110–1119, 2021.

[28] R. Merletti and G. L. Cerone, "Tutorial. Surface EMG detection, conditioning and pre-processing: Best practices," *J. Electromyogr. Kinesiol.*, vol. 54, Oct. 2020, Art. no. 102440, doi: 10.1016/j.jelekin.2020.102440.

[29] G. L. Cerone, A. Botter, and M. Gazzoni, "A modular, smart, and wearable system for high density sEMG detection," *IEEE Trans. Biomed. Eng.*, vol. 66, no. 12, pp. 3371–3380, Dec. 2019, doi: 10.1109/TBME.2019.2904398.

[30] A. Botter and T. M. Vieira, "Filtered virtual reference: A new method for the reduction of power line interference with minimal distortion of monopolar surface EMG," *IEEE Trans. Biomed. Eng.*, vol. 62, no. 11, pp. 2638–2647, Nov. 2015, doi: 10.1109/TBME.2015.2438335.

[31] A. Holobar and D. Zazula, "Multichannel blind source separation using convolution kernel compensation," *IEEE Trans. Signal Process.*, vol. 55, no. 9, pp. 4487–4496, Sep. 2007.

[32] A. Holobar, M. A. Minetto, A. Botter, F. Negro, and D. Farina, "Experimental analysis of accuracy in the identification of motor unit spike trains from high-density surface EMG," *IEEE Trans. Neural Syst. Rehabil. Eng.*, vol. 18, pp. 221–229, 2010, doi: 10.1109/TNSRE.2010.2041593.

[33] A. D. Vecchio, A. Holobar, D. Falla, F. Felici, R. M. Enoka, and D. Farina, "Tutorial: Analysis of motor unit discharge characteristics from high-density surface EMG signals," *J. Electromyogr. Kinesiol.*, vol. 53, Aug. 2020, Art. no. 102426, doi: 10.1016/j.jelekin.2020.102426.

[34] K. E. Power, E. J. Lockyer, A. Botter, T. Vieira, and D. C. Button, "Endurance-exercise training adaptations in spinal motoneurones: Potential functional relevance to locomotor output and assessment in humans," *Eur. J. Appl. Physiol.*, vol. 122, no. 6, pp. 1367–1381, Jun. 2022, doi: 10.1007/s00421-022-04918-2.

[35] W. Troni, R. Cantello, and I. Rainero, "Conduction velocity along human muscle fibers in situ," *Neurology*, vol. 33, no. 11, pp. 1453–1458, Nov. 1983, doi: 10.1212/wnl.33.11.1453.

[36] R. Merletti, D. Farina, and M. Gazzoni, "The linear electrode array: A useful tool with many applications," *J. Electromyogr. Kinesiol.*, vol. 13, no. 1, pp. 37–47, Feb. 2003.

[37] D. F. Stegeman, D. Dumitru, J. C. King, and K. Roeleveld, "Near- and far-fields: Source characteristics and the conducting medium in neurophysiology," *J. Clin. Neurophysiology*, vol. 14, no. 5, pp. 429–442, Sep. 1997, doi: 10.1097/00004691-199709000-00009.

[38] R. Merletti, A. Botter, A. Troiano, E. Merlo, and M. A. Minetto, "Technology and instrumentation for detection and conditioning of the surface electromyographic signal: State of the art," *Clin. Biomechanics*, vol. 24, no. 2, pp. 122–134, Feb. 2009, doi: 10.1016/j.clinbiomech.2008.08.006.

[39] S. Huang et al., "Flexible tongue electrode array system for in vivo mapping of electrical signals of taste sensation," *ACS Sensors*, vol. 6, no. 11, pp. 4108–4117, Nov. 2021, doi: 10.1021/acssensors.1c01621.

[40] C. Wang et al., "Stretchable, multifunctional epidermal sensor patch for surface electromyography and strain measurements," *Adv. Intell. Syst.*, vol. 3, no. 11, pp. 1–32, Nov. 2021, doi: 10.1002/aisy.202100031.

[41] D. H. Lee, T. Park, and H. Yoo, "Biodegradable polymer composites for electrophysiological signal sensing," *Polymers*, vol. 14, no. 14, p. 2875, Jul. 2022, doi: 10.3390/polym14142875.

[42] L. Mu and I. Sanders, "Human tongue neuroanatomy: Nerve supply and motor endplates," *Clin. Anatomy*, vol. 23, no. 7, pp. 777–791, Oct. 2010, doi: 10.1002/ca.21011.

[43] S. Buchaillard, M. Brix, P. Perrier, and Y. Payan, "Simulations of the consequences of tongue surgery on tongue mobility: Implications for speech production in post-surgery conditions," *Int. J. Med. Robot. Comput. Assist. Surgery*, vol. 3, no. 3, pp. 252–261, Sep. 2007, doi: 10.1002/rcs.142.

[44] V. Vacchiano et al., "Prognostic value of EMG genioglossus involvement in amyotrophic lateral sclerosis," *Clin. Neurophysiol.*, vol. 132, no. 10, pp. 2416–2421, Oct. 2021, doi: 10.1016/j.clinph.2021.07.011.

[45] S. Misawa et al., "Ultrasonographic detection of fasciculations markedly increases diagnostic sensitivity of ALS," *Neurology*, vol. 77, no. 16, pp. 1532–1537, Oct. 2011, doi: 10.1212/wnl.0b013e318233b36a.

[46] M. de Carvalho et al., "Electrodiagnostic criteria for diagnosis of ALS," *Clin. Neurophysiol.*, vol. 119, no. 3, pp. 497–503, Mar. 2008, doi: 10.1016/j.clinph.2007.09.143.

[47] A. Tamborska et al., "Non-invasive measurement of fasciculation frequency demonstrates diagnostic accuracy in amyotrophic lateral sclerosis," *Brain Commun.*, vol. 2, no. 2, Sep. 2020, Art. no. fcaa141, doi: 10.1093/braincomms/fcaa141.

[48] P. Zhou, X. Li, F. Jahanmiri-Nezhad, W. Rymer, and P. E. Barkhaus, "Duration of observation required in detecting fasciculation potentials in amyotrophic lateral sclerosis using high-density surface EMG," *J. NeuroEngineering Rehabil.*, vol. 9, no. 1, p. 78, 2012, doi: 10.1186/1743-0003-9-78.

[49] A. Botter, M. Carbonaro, T. M. Vieira, and E. Hodson-Tole, "Identification of muscle fasciculations from surface EMG: Comparison with ultrasound-based detection," in *Proc. 41st Annu. Int. Conf. IEEE Eng. Med. Biol. Soc. (EMBC)*, Jul. 2019, pp. 5117–5120, doi: 10.1109/EMBC.2019.8857873.

[50] M. Crook-Rumsey et al., "A shortened surface electromyography recording is sufficient to facilitate home fasciculation assessment," *Muscle Nerve*, vol. 66, no. 5, pp. 625–630, Nov. 2022, doi: 10.1002/mus.27701.

Open Access funding provided by 'Politecnico di Torino' within the CRUI CARE Agreement